



## Experimental study of spruce wood reaction to fire in single burning item test

Lucas Terrei, Davood Zeinali, Zoubir Acem, Véronique Marchetti, Paul Lardet, Pascal Boulet, Gilles Parent

### ► To cite this version:

Lucas Terrei, Davood Zeinali, Zoubir Acem, Véronique Marchetti, Paul Lardet, et al.. Experimental study of spruce wood reaction to fire in single burning item test. *Journal of Fire Sciences*, 2022, 40 (4), pp.293-310. 10.1177/07349041221089829 . hal-04454807

**HAL Id: hal-04454807**

**<https://hal.science/hal-04454807>**

Submitted on 13 Feb 2024

**HAL** is a multi-disciplinary open access archive for the deposit and dissemination of scientific research documents, whether they are published or not. The documents may come from teaching and research institutions in France or abroad, or from public or private research centers.

L'archive ouverte pluridisciplinaire **HAL**, est destinée au dépôt et à la diffusion de documents scientifiques de niveau recherche, publiés ou non, émanant des établissements d'enseignement et de recherche français ou étrangers, des laboratoires publics ou privés.

## EXPERIMENTAL STUDY OF SPRUCE WOOD REACTION TO FIRE IN SINGLE BURNING ITEM TEST

Journal:	<i>Journal of Fire Sciences</i>
Manuscript ID	JFS-21-0112.R1
Manuscript Type:	Original Research Article
Date Submitted by the Author:	n/a
Complete List of Authors:	T, Lucas; LEMTA, Zeinali, Davood; LEMTA Acem, Zoubir; LEMTA Marchetti, Véronique; CSTB Lardet, Paul; CSTB Boulet, Pascal; Université de Lorraine, LEMTA Parent, Gilles; LEMTA
Keywords:	Single Burning Item, Cone calorimeter, Wood degradation
Abstract:	The aim of this work is to study and characterize the fire behavior of vertically-oriented spruce wood panels using experiments conducted at the scales of cone calorimeter and Single Burning Item (SBI) tests. Wood panels were exposed to different burner powers for three exposure times. Very thin thermocouples were embedded inside the wood panel to measure the in-depth temperatures while the lateral position of the char front on the exposed surface and the depth of the char layer were also measured for each test. The latter measurement permitted to establish a char depth map according to the burner power and exposure time. It was observed that for a fixed exposure time, the degraded area on the surface grows linearly with the burner power. Finally, a comparison is made between the char front depths measured with the SBI and those measured with the cone calorimeter for similar heat fluxes.

SCHOLARONE™  
Manuscripts

# EXPERIMENTAL STUDY OF SPRUCE WOOD REACTION TO FIRE IN SINGLE BURNING ITEM TEST

Lucas TERREI<sup>a,\*</sup>, Davood ZEINALI<sup>a</sup>, Zoubir ACEM<sup>a</sup>, Véronique MARCHETTI<sup>b</sup>, Paul LARDET<sup>b</sup>,  
Pascal BOULET<sup>a</sup>, Gilles PARENT<sup>a</sup>

<sup>a</sup>Université de Lorraine, CNRS, LEMTA, F-54000 Nancy, France

<sup>b</sup>Université Paris-Est, Centre Scientifique et Technique du Bâtiment (CSTB), France

## Abstract

The aim of this work is to study and characterize the fire behavior of vertically-oriented spruce wood panels using experiments conducted at the scales of cone calorimeter and Single Burning Item (SBI) tests. For this purpose, firstly incombustible panels were exposed to burner powers of 15, 20, 30 and 50 kW in the SBI tests to obtain a mapping of the total heat fluxes received by the panel. Subsequently, wood panels were exposed to the same burner powers for exposure times of 15, 20 and 30 minutes. Very thin thermocouples were embedded inside the wood panel to measure accurately the in-depth temperatures while the lateral position of the char front on the exposed surface and the depth of the char layer were also measured for each test. The latter measurement permitted to establish a char depth map according to the burner power and exposure time. Correspondingly, it was observed that for a fixed exposure time, the degraded area on the surface grows linearly with the burner power. Moreover, the in-depth char front position deduced from the 300 °C isotherm was found to comply very well with that obtained from direct measurements. Finally, a comparison is made between the char front depths measured with the SBI and those measured with the cone calorimeter for similar heat fluxes, showing that the corresponding charring rates from these two tests deviate from one another only at low heat fluxes.

**Keywords:** Single Burning Item, cone calorimeter, wood, degradation

## INTRODUCTION

In Europe, building materials are subjected to standardized tests which allow classification according to their reaction to fire.<sup>1</sup> One of the most widely used tests in reaction to fire is the Single Burning Item (SBI).<sup>2</sup> The SBI test is an intermediate-scale test between bench-scale tests such as Fire Propagation Apparatus (FPA) test and full-scale test such as ISO Room Corner test.<sup>3</sup> This test simulates a single burning

\*Corresponding author: lucas.terrei@univ-lorraine.fr

item at the bottom of a room corner (like a burning trashcan) using a propane burner to test construction products and to classify them according to their fire reaction. The performance is evaluated over a period of 20 minutes with visual and non-visual observations. During the experiment, visual observations are recorded regarding the horizontal spread of the flame front and the fall of flaming droplets or particles. Non-visual measurements such as the Heat Release Rate (HRR) are mainly evaluated with oxygen and carbon dioxide analyzers. Other measurements such as CO or smoke are also possible with the SBI. According to the results, the materials are then classified into predefined European classes. For this normative test, the HRR provided by the burner is fixed at  $30 \pm 2$  kW, which is restrictive for studying the fire behavior of samples at this intermediate-scale. Beyond the normative framework of this test, the SBI could be useful to study how wood or other materials behave at the intermediate scale (i.e. between the cone calorimeter<sup>4</sup> and the room corner test<sup>3</sup>), varying the experimental conditions, such as the burner power or the exposure time.

A recent study performed by Zeinali *et al.*<sup>5</sup> characterizes the SBI gas burner against incombustible calcium silicate panels. In that study, data is provided regarding the flame height, total heat fluxes and panel temperatures measured at burner powers of 10, 30, and 55 kW. They observed that the flame height of the burner and the measured heat flux increased with the imposed power. Moreover, they showed that the thermal stress produced by the SBI gas burner over the surface of the panels is non-uniform. Zhang *et al.*<sup>6</sup> conducted similar experiments with incombustible panels and measured the burner heat fluxes on the walls as well as the burner flame heights and the conclusions were similar to those of Zeinali *et al.*<sup>5</sup> More specifically, Zhang *et al.*<sup>6</sup> reported mean flame heights of 0.81 m and 1.19 m for the burner powers of 30 kW and 55 kW, respectively, while Zeinali *et al.*<sup>5</sup> reported flame heights of 0.87 m and 1.12 m for the same burner powers. Zeinali *et al.*<sup>7</sup> have also studied the fire behavior of Medium Density Fiberboard (MDF) panels with a 30 kW burner power. Flame heights were measured and it was observed that the presence of a combustible panel increases the flame height as well as the HRR compared to tests with calcium silicate panels. The propagation of the char front over the surface of the MDF panels was also measured as a function of the exposure time for 30 kW burner power. Lipinskas and Mačiulaitis<sup>8</sup> performed tests with the SBI to compare the charring rate of different wood samples (hardwood and softwood, treated and untreated). They showed that this speed can vary from 0.5 to 0.8 mm. min<sup>-1</sup> for a burner power of 30 kW. Among the 4 types of wood samples, it was observed that the density of the wood (and not the treatment) has the major influence on the char production.

1  
2  
3  
4  
5  
6  
7  
8  
9  
10  
11  
12  
13  
14  
15  
16  
17  
18  
19  
20  
21  
22  
23  
24  
25  
26  
27  
28  
29  
30  
31  
32  
33  
34  
35  
36  
37  
38  
39  
40  
41  
42  
43  
44  
45  
46  
47  
48  
49  
50  
51  
52  
53  
54  
55  
56  
57  
58  
59  
60

Many works have studied how the experimental scale changes the fire behavior of materials.<sup>9, 10, 11, 12, 13, 14</sup> The Research Institute of Sweden (formerly SP) tried to correlate the results of cone calorimeter with those of room corner and SBI test using, in the basis of HRR and smoke production.<sup>9</sup> They developed a specific software (Cone Tools) in order to calculate the HRR and the smoke parameters in SBI and room corner tests from the cone calorimeter results. In other experiments, Hansen and Hovde<sup>10</sup> as well as Delichatsios,<sup>11</sup> used ignition times estimated from the cone calorimeter test to predict the flashover time in the ISO Room Corner test. Hakkarainen and Kokkala<sup>12</sup> evaluated the HRR evolution of a material in the early stages of the experiment in the Room Corner test, thanks to the HRR measured with a cone calorimeter at 50 kW.m<sup>-2</sup>. Axelsson *et al.*<sup>13</sup> showed that the errors related to the determination of HRR in SBI and Room Corner tests are nearly 10 %, discussing data conventionally obtained from SBI tests such as the Fire Growth RATE (FIGRA), the Total Heat Release (THR) and the SMOke Growth RATE (SMOGRA) on sandwich panels.<sup>14</sup> They concluded that “the correlation between full-scale behaviour in the used set-ups and the new SBI data is still not satisfactory”, showing the need for more research to improve understanding of scale changing. Tsantaridis<sup>15</sup> studied the reaction to fire of wood and building products according to tests at different scale. A single comparison if the FIGRA between the SBI test and the cone calorimeter test (with a constant heat flux of 50 kW.m<sup>-2</sup>) was performed. A linear correlation was identified even if this correlation should be confirmed with additional experiments. Despite the significant use of SBI for the classification of building materials, recent research concerning wood products at this scale remains insufficient. At SBI scale, most of the studies are based on the comparison between different wood samples with a burner power fixed at 30 kW.<sup>7, 8</sup> Previous studies showed that the comparisons between cone calorimeter and SBI tests were mainly addressed in the basis of HRR and smoke productions. However, few data are available regarding others properties like in-depth temperatures or surface and in-depth char front mapping. In the present work, the SBI test was used beyond its normative framework in order to study and characterize the fire behavior of vertically-oriented spruce wood panels. The tests were conducted with burner powers of 15, 20, 30 and 50 kW, for exposure times of 15, 20 and 30 minutes, while the propagation of the char front on the exposed surface and the depth of char in the panels were measured. For the tests carried out at 30 kW, thin wire thermocouples embedded in the wood sample were used to measure accurately the in-depth temperature as described in Terrei *et al.*<sup>16</sup> In this paper, the results obtained with this method were compared with in-depth temperatures measured by sheathed thermocouples

to show the benefit of such an implantation.

The distribution of the total heat fluxes over the surface of the panels was quantified for all the burner powers on incombustible panels using total fluxmeter. Subsequently, the location with the highest heat flux was determined and chosen to make a comparison against the heat fluxes of tests with spruce wood panels. Finally the char depth measured in the SBI tests was compared to that obtained from cone calorimeter tests.

## EXPERIMENTAL SETUP

### *The SBI*

A total of 22 experiments were conducted with the SBI setup<sup>2</sup> using spruce wood with an exposed surface area of 150 cm by 50 cm. Wood samples were glulam panels made with ten battens of spruce wood glued together with melamine-urea-formaldehyde (MUF) resin. The batten section was 5 × 5 cm, so the panel was 5 cm thick, that can be considered to be thermally thick. The sample average density was approximately 490 kg.m<sup>-3</sup>, with an average moisture content of nearly 10 %. Wood panels were stored in a temperature and humidity controlled room. The SBI consists of a frame on which two vertical panels of the studied material are perpendicularly arranged. A propane sand box burner is placed at 4 cm from the corner. The burner is an isosceles right-angled triangle with 25 cm side. The setup is placed in a dedicated test room (3 m × 3 m × 2.4 m), under a hood with a system to continuously extract a flow rate from 0.50 to 0.65 m<sup>3</sup>.s<sup>-1</sup>.

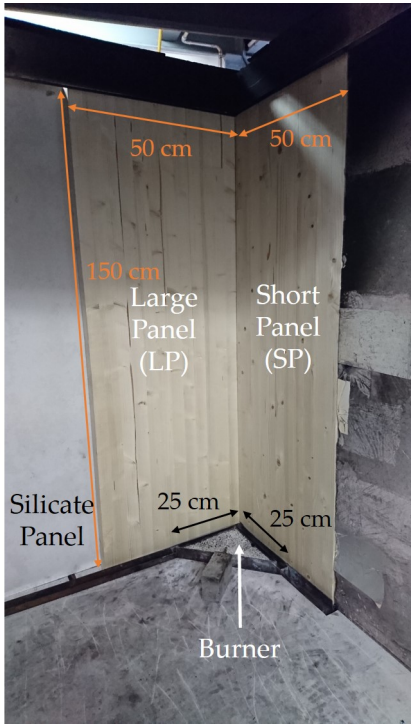


Figure 1: SBI experimental setup.

For the normative test, the two panels exposed to the burner do not have the same dimension. There are one short panel (50 cm × 150 cm) and one large panel (100 cm × 150 cm). This arrangement makes it possible to observe the horizontal spread of the flame during the test. Nevertheless, it was shown by Zeinali *et al.*<sup>7</sup> that the flame spread on the long MDF panel never exceeds 50 cm, i.e. less than the short panel width. So, for this study, two identical panels having a 50 cm width were used. A similar configuration was also chosen by Chaudhari *et al.* on PMMA panels.<sup>17</sup> Additionally, in the present configuration, the remainder of the wall on the large panel side was completed by a 50 cm wide calcium silicate panel to remain in the same configuration to the original SBI test and ensure an air supply similar to the tests carried out in previous works. For the sake of clarity, the labels “large panel” and “short panel” denominations will be still used in the paper as shown in Fig. 1. The spruce panels were exposed to burner HRR values of 15, 20, 30 and 50 kW for exposure times of 15, 20 and 30 minutes. Temperatures inside the wood were measured with K-type thermocouples during the tests. However, depending on how the thermocouples are implanted in the wood sample, the measured temperature can vary by up to 400 °C for some experimental conditions, as shown in.<sup>16, 18, 19</sup> A precise measurement method was developed recently,<sup>16</sup> consisting in embedding very thin (0.1 mm diameter) wire thermocouples in-



side the sample, along the isotherms parallel to the exposed surface. This method was validated at the small scale with cone calorimeter tests and is implemented here, at the SBI scale. For that, the wood panel was cut perpendicularly to the exposed surface, and then square-grooves with 0.2 mm depth and 0.2 mm width were precisely machined at the desired locations. Then, wire K-type thermocouples composed of alumel and chromel wires were welded by autogenous electric welding and put in the square-grooves. Finally, wood panel was glued with Melamine-Urea-Formaldehyde (MUF). More details concerning the protocol of the thermocouple implantation in the wood sample are presented in.<sup>16</sup> At the scale of SBI, implanting the thermocouple wires in this way takes four hours per sample from grooving to bonding and thermocouple welding. The temperature was only studied for the short panel. Figure 2 shows the position of the thermocouples in the wood sample. The thermocouple junctions (red points in Fig. 2) are placed at 9 cm from the corner line and 45 cm from the bottom of the panel, at a location where the panel should be severely affected by the burner flame.

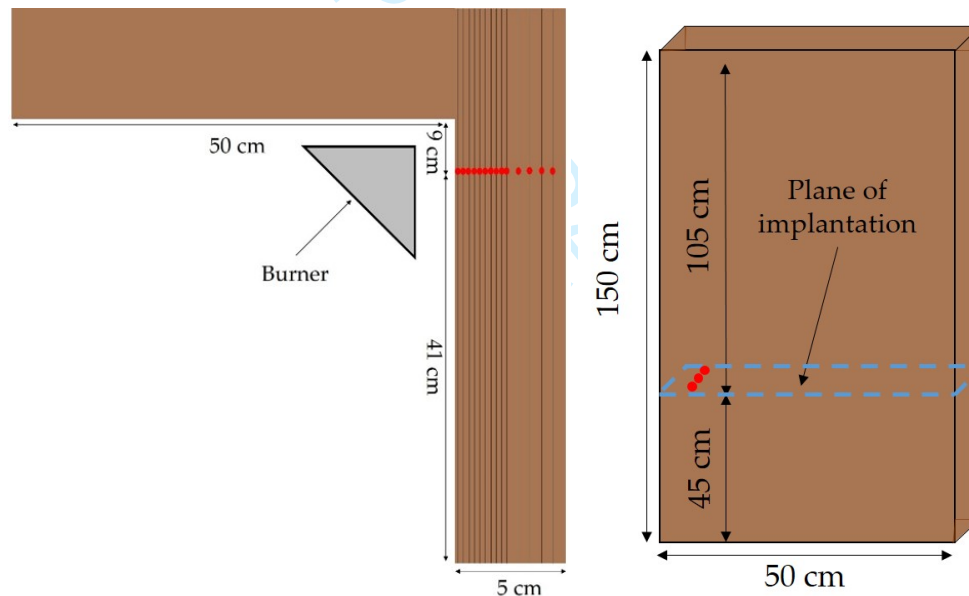


Figure 2: Diagrams showing the in-depth thermocouple measurement points (red circles) inside the wood panel. The top view of the panel is shown to the left, while the side view of the measurement panel is shown to the right.

To verify the importance of how the thermocouples are implanted in the wood sample and assess discrepancies, separate tests were also performed with four K-type sheathed thermocouples (1 mm diameter) placed inside holes drilled on the back side of the sample (i.e., perpendicular to the isotherms) using a 1.5 mm diameter drill bit, respectively at 10, 20, 30 and 40 mm depth from the exposed surface. As



1  
2  
3  
4  
5  
6  
7  
8  
9  
10  
11  
12  
13  
14  
15  
16  
17  
18  
19  
20  
21  
22  
23  
24  
25  
26  
27  
28  
29  
30  
31  
32  
33  
34  
35  
36  
37  
38  
39  
40  
41  
42  
43  
44  
45  
46  
47  
48  
49  
50  
51  
52  
53  
54  
55  
56  
57  
58  
59  
60

suggested by Reszka and Torero,<sup>20</sup> the sheathed thermocouples were spaced by 20 mm in order to limit their mutual disturbance.

***The cone calorimeter***

As introduced by previous studies,<sup>10,11,12</sup> comparisons between the cone calorimeter<sup>4</sup> and the SBI<sup>2</sup> are very useful for the understanding of the fire behavior of materials. The HRR evolution or the time-to-ignition are among the most often used data to identify the correlation between the two scales. In the present work, the char depth positions in the two scales were compared over time. Following the standard ISO 5660-1, the wood samples in the cone calorimeter tests were wrapped with two layers of aluminum foil, and the distance between the heater and the tested samples was 25 mm. For these experiments, the cone heater and wood samples were oriented vertically like for SBI tests, without a pilot flame or spark. The spruce wood material of the cone samples (10 cm × 10 cm × 5 cm) was identical to that tested at intermediate scale. The incident heat fluxes for the cone calorimeter tests were chosen in order to match the SBI heat fluxes measured both with the wood and the incombustible panels.

**RESULTS**

This section firstly presents the results of the SBI tests conducted with incombustible calcium silicate panels (average density: 870 ±50 kg.m<sup>-3</sup> and 12 mm thickness), followed by the test results of spruce wood panels in SBI and the cone calorimeter, discussing the heat fluxes, in-depth temperatures, char front on the exposed surface and char front depth in the samples.

***Total incident heat fluxes on incombustible panels in SBI***

First, an inert calcium silicate panel was exposed to the burner powers equal to 15, 20, 30 and 50 kW, while the total incident heat fluxes were measured with a water-cooled (around 12 °C) heat flux gauge (Gardon type from Captec). This heat flux sensor was placed in holes with a diameter equal to that of the fluxmeter (i.e., 2.5 cm), previously drilled on the short panel at various locations. Figure 3 shows the locations of the gauge and the corresponding mapping of the measured heat fluxes for different burner powers. The free holes were blocked with plugs from the same materials as the panel to prevent any gas flow through them. The heat flux was measured on the small panel at a total of 22 points with locations ranging from 15 to 105 cm along the height and from 0 to 40 cm along the width. For each burner power and measurement point, the heat flux was recorded for 2 minutes. When the burner is ignited, it is

necessary to wait for approximately 30 seconds before reaching a steady state. As a result, the average of the flux value and its standard deviation were only calculated for the last 90 seconds. The acquisition frequency being 5 Hz, the average was taken over approximately 365 measurements. Figure 3 presents a map of the heat fluxes obtained for each burner power.

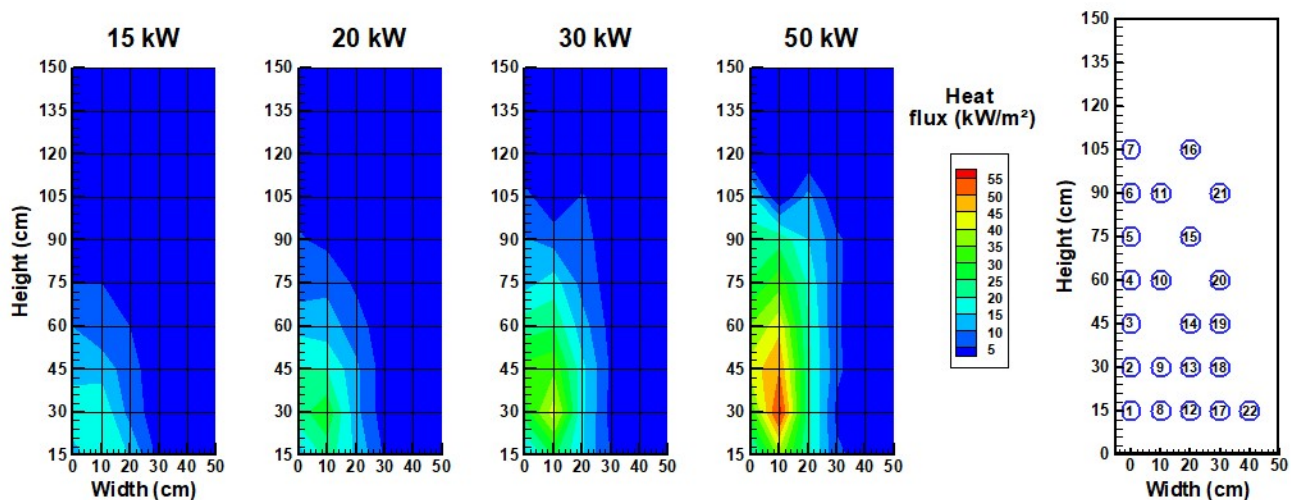


Figure 3: Contour plots of total heat fluxes obtained using burner powers of 15, 20, 30 and 50 kW on the incombustible short panel. The measurements were made using a water-cooled heat fluxmeter at the locations shown on the diagram to the right.

The heat flux maps illustrated in Fig. 3 show that the heat flux received at the wall increases locally with the power of the burner. For a 50 kW burner power, the measured heat flux is at least  $30 \text{ kW} \cdot \text{m}^{-2}$  over a large area (20 cm wide and 85 cm high). Beyond 105 cm in height and 30 cm in width, the heat flux was not measured (except in position 22) but the heat flux does not exceed  $5 \text{ kW} \cdot \text{m}^{-2}$  there. These measurements are consistent with those obtained in Zhang *et al.*<sup>6</sup> and Zeinali *et al.*<sup>5</sup> works showing the heterogeneity of the irradiance over the sample surface.

#### ***Total incident heat fluxes on the spruce wood panel***

The same fluxmeter used in the previous section was placed at position 9 shown in Fig. 3, i.e. at a height of 30 cm and a distance of 10 cm from the corner in order to measure the heat flux on the spruce wood panel for the burner powers of 15, 20, 30 and 50 kW. It will be possible to observe the additional effect of the flame produced by the burning wood by comparing the heat flux received by the two types of sample. Figure 4 shows the values of the measured heat fluxes as a function of the imposed burner power. The heat fluxes in the wood panel tests were averaged over 15 minutes of testing.

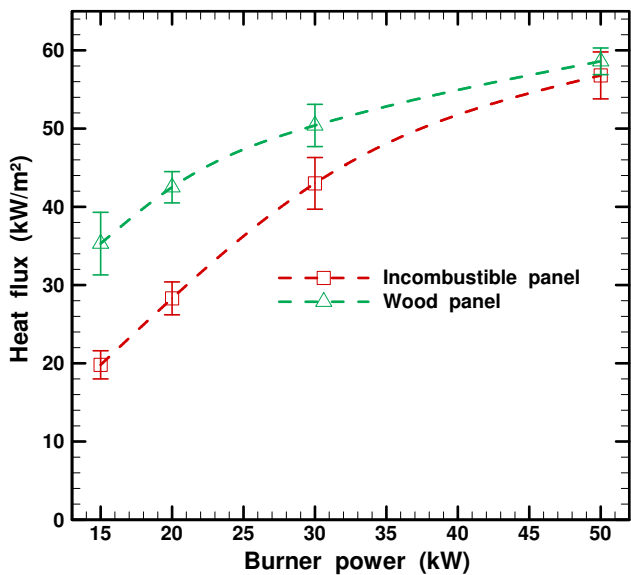


Figure 4: Comparison of the total incident heat fluxes measured on an incombustible panel (squares) and that with a spruce wood panel (triangles) as a function of the burner power.

The measurements indicate that the heat flux received by the wooden panel is systematically higher than that received by the incombustible panel for the same burner powers (see Fig.4). For a 15 kW burner power, the heat flux is increased by 85 % for the wood panel, compared to the inert panel, but only 3 % for the 50 kW burner power. This shows that the difference tends to decrease as the heating power increases. Indeed, for a low power of the burner, the heat flux received on the panels is mainly radiative since the burner flame is too small to stick to the panel surface (more precisely at the fluxmeter's location). For a combustible panel, the burning of the panel produces an additional convective heat flux on the panel surface, as the pyrolysis gases feed and widen the burner flame. Therefore, the heat fluxes received by the combustible panels are significantly larger than those received by the inert panels. This explains the large differences in the irradiance of the two types of surface for the 15 and 20 kW tests. For higher burner powers, the flame of the burner is large enough to stick to the panel surface so a convective flux coming from the burner flame is also present. In this case, the pyrolysis gases feed the burner flame but its thickness does increase any further. Moreover, the combustible panels in this case also experience the so-called “blowing effect”, i.e., reduction of convective heat transfer to the surface due to the opposite flow of pyrolyzate mass.<sup>5,21,22</sup> Accordingly, as the burning rate of the panels increases with higher burner powers, the convective heat transfer to the surface decrease, just as reported in.<sup>7,23</sup> This

explains the convergence of the heat fluxes of combustible and incombustible panel tests as the burner power increases at the position where the heat flux was measured.

### *Surface char front propagation on the wood panels*

After each test, the wood panels were extinguished with water in order to stop the wood combustion and degradation. The inspection of the samples after the tests shows that the power of the burner plays an important role in the degradation of the wood. Figure 5 presents spruce wood samples after tests at different burner powers for an exposure time of 15 minutes. For the same exposure time, the quantity of char increases with the imposed power.



Figure 5: Photos of test specimens after 15 minutes of testing with burner powers ranging from 15 to 50 kW.

As illustrated in Fig. 5, it is possible to define three zones of degradation: (A) the zone next to the corner line formed by the panels, severely degraded with millimeter-sized cracks (zone A always has char depths higher than 9 mm); (B) the intermediate zone between the region with large cracks and the region with no significant cracks (zone B has char depths between 2 and 9 mm); (C) the charred zone farthest away from the corner line, featuring a minimum level of degradation and no significant cracks (zone C has char depths between 0 and 1 mm). The width of these three zones were measured for each panel every 20 cm along the height. Figure 6 presents the boundaries of zones A, B and C on a test specimen for three tests performed at 20 kW for 30 minutes.



1  
2  
3  
4  
5  
6  
7  
8  
9  
10  
11  
12  
13  
14  
15  
16  
17  
18  
19  
20  
21  
22  
23  
24  
25  
26  
27  
28  
29  
30  
31  
32  
33  
34  
35  
36  
37  
38  
39  
40  
41  
42  
43  
44  
45  
46  
47  
48  
49  
50  
51  
52  
53  
54  
55  
56  
57  
58  
59  
60

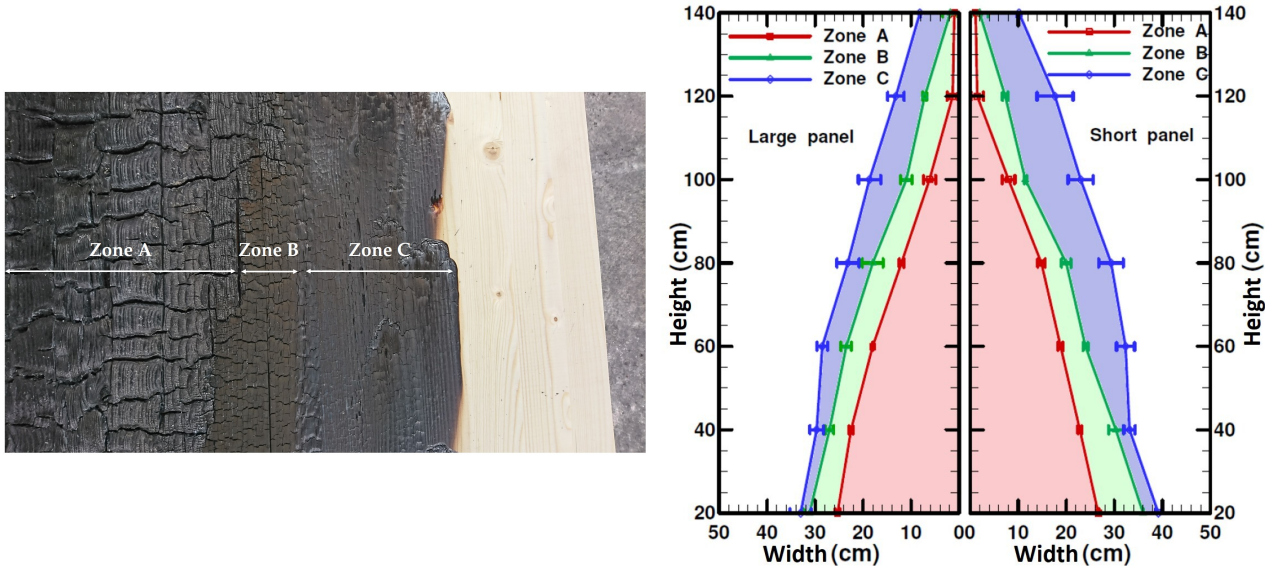


Figure 6: Degradation zones of wood samples for tests conducted with a 20 kW burner power. The error bars indicate the magnitude of one standard deviation across the tests.

Figure 6 also indicates the standard deviation in the positioning of the boundaries of zones A, B and C in the three tests carried out with the spruce wood panels. We can see that the location of zone A is quite repeatable (small error bars) whereas more discrepancies are observed on boundaries of zones B and C. Figure 7 presents the propagation of the char front over the surface in zone A as a function of the burner power for two exposure times, namely 15 and 30 minutes.

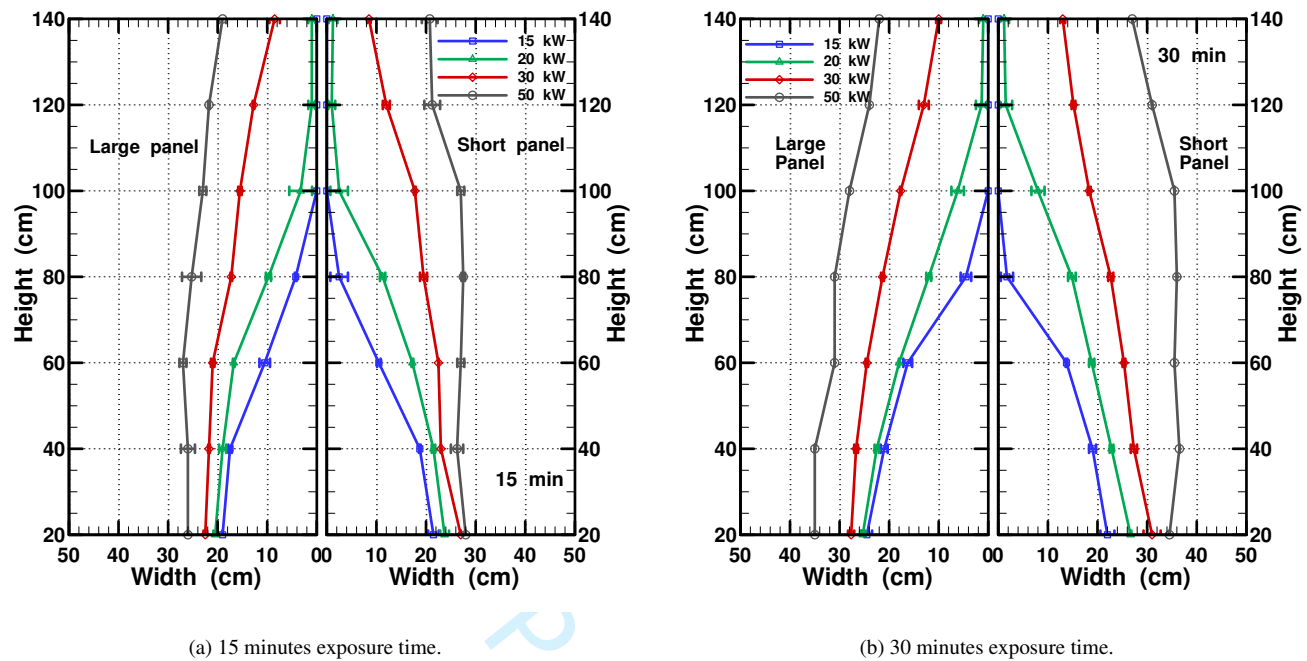


Figure 7: Evolution of the surface char front in zone A for different burner powers with exposure times of 15 min (left) and 30 min (right). The error bars indicate the magnitude of one standard deviation across three tests.

For a given exposure time, the propagation of the char front at the surface increases with the burner power. There is also an asymmetry between the degradation patterns of the short panel and those of the large panel. This observation is also confirmed by the char depth, which generally shows that the short panel is more degraded than the large one. This observation concerning the in-depth temperatures and heat fluxes was also observed by Zeinali *et al.*<sup>5</sup> and Zhang *et al.*,<sup>6</sup> and is expected to be due to the air supply pattern in the setup which favors flame spread on the short panel.<sup>23</sup> Indeed, this phenomenon leads to higher temperatures of 100 °C<sup>5</sup> as well as 1 to 5 kW.m<sup>-2</sup> larger heat fluxes<sup>6</sup> on the short side.

Figure 8 shows how the area of zone A increases as a function of the imposed burner power.

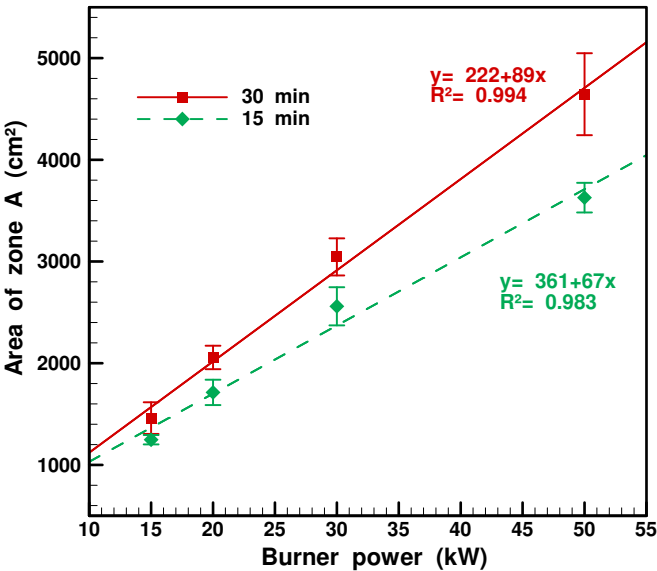


Figure 8: Evolution of the area of zone A as a function of the burner power. The error bars indicate the magnitude of one standard deviation across three experiments.

For a given exposure time, the area of zone A increases almost linearly with the burner power. In other words, the surface of degradation is almost doubled when the burner power is multiplied by two. On the other hand, doubling the exposure time for the burner powers of 15, 30 and 50 kW increases the degradation area of zone A by 15, 20 and 30 %, respectively. This means that the area of zone A does not increase linearly with the exposure time.

***In-depth panel temperatures***

Figure 9 presents the temperature evolutions for the different depths. The tests were carried out three times for a 30 kW burner power.



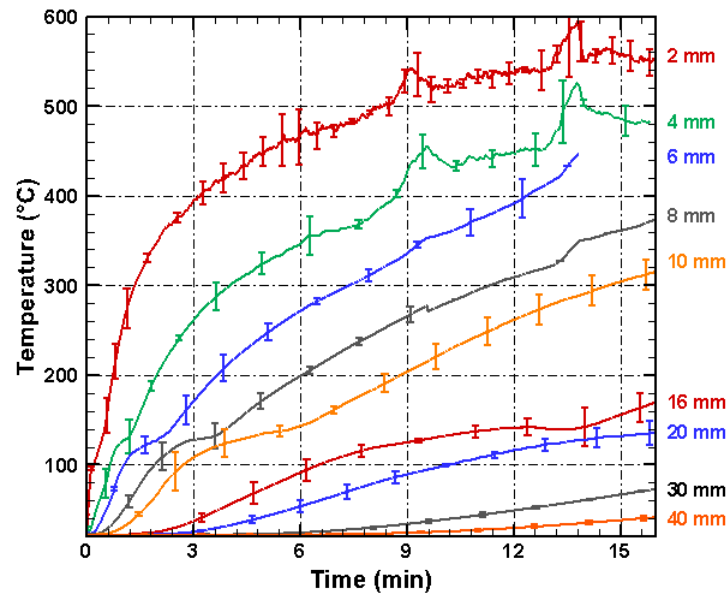


Figure 9: In-depth temperature evolutions measured by embedded wire thermocouples located at 2 to 40 mm depth from the exposed surface for a 30 kW burner power. The error bars indicate the magnitude of one standard deviation across three tests.

On the side exposed to the burner, the in-depth panel temperatures increase rapidly before reaching a slower growing phase. The small error bars, corresponding to the standard deviation values, suggest that the repeatability of the tests is sufficient. At 2 mm depth, the error bars are larger due to the fast heating dynamics. The maximum temperature is 600 °C. Two peaks are present at depths of 2 and 4 mm at exposure times of 9 and 14 minutes, possibly due to the appearance of an incandescent zone close to the measurement sensor. Moreover, there is also an inflection around 120 °C just as observed in cone calorimeter tests.<sup>16</sup> Figure 10 compares the results obtained at the different depths with the sheathed thermocouples (oriented perpendicular to the panel's exposed surface) and the wire thermocouples (oriented parallel to the panel's exposed surface).

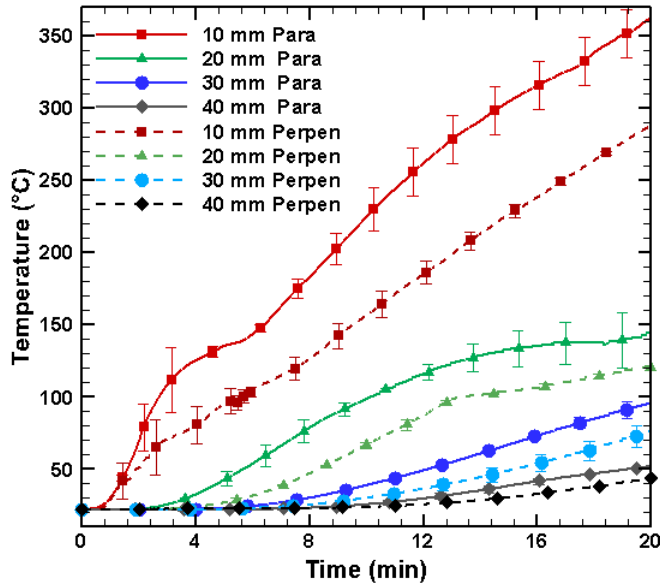


Figure 10: In-depth panel temperatures measured using sheathed thermocouples placed in holes drilled from the back of the panel (dashed lines) and those measured using bare thermocouple wires placed parallel to the isotherms by implantation (solid lines), in tests with a burner power of 30 kW.

As Fig. 10 indicates, the temperature measurements made with sheathed thermocouples placed in holes drilled from the back side show significant differences from the temperatures obtained using bare thermocouple wires implanted along the isotherms. This is the case even for positions that are far from the exposed surface. The temperature at the end of the test at 10 mm depth is 360 °C for the embedded thermocouple against 285 °C for the sheathed thermocouple, i.e., a 75 °C difference. At the depth of 10 mm, it takes more than 6 minutes delay for the two types of thermocouple to record 300 °C (14 minutes for the embedded thermocouple and more than 20 minutes for the sheathed thermocouple). The differences are smaller at 20, 30 and 40 mm depths but still significant.

### Char front propagation

Several additional specimens were exposed to 30 kW for 15, 20 and 30 minutes before being cut in half at the thermocouple junctions location (45 cm height and 9 cm from the corner). At this location, the heat flux received is around 35 kW.m<sup>-2</sup> according to Fig. 3, which can be used to make comparisons with cone tests<sup>16</sup> in terms of charring rates. Correspondingly, the char front depth of the panels was measured at this location with a ruler and was compared with the position of the 300 °C isotherm (determined from

258 embedded thermocouples temperature measurements).<sup>16,24</sup> The results are presented in Fig. 11.

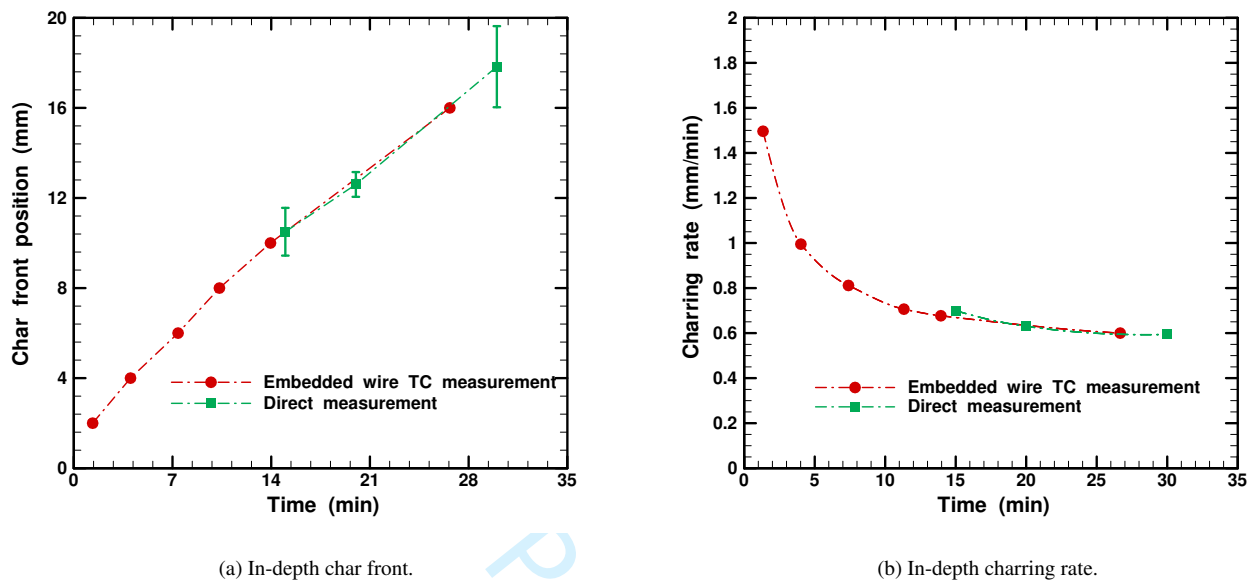


Figure 11: Comparison of the in-depth char front propagation (left) and the deduced charring rate (right), determined either on direct measurements of the char layer thickness (square symbols) or estimated by the 300 °C isotherm measurements made using the embedded thermocouples (circle symbols), with a burner power of 30 kW.

259 The in-depth char front positions determined via direct measurements are in good agreement with  
 260 those estimated by the 300 °C isotherm measurements made using the embedded thermocouples, just  
 261 as observed by Terrei *et al.*<sup>16</sup> The char front reached the depths of 10.5 and 18 mm after the exposure  
 262 times of 15 and 30 min, respectively. It appears that the propagation of the char front slows down with  
 263 time according to a power law, as showed in Fig. 11b. The curve shows that the charring rate is not  
 264 constant during the experiment. It starts at 1.5 mm.min<sup>-1</sup> and decreases rapidly to 0.7 mm.min<sup>-1</sup> after  
 265 10 minutes of exposure. Subsequently, the charring rate becomes more or less constant, staying between  
 266 0.6 and 0.7 mm.min<sup>-1</sup>, and such values comply well with those obtained in previous studies performed  
 267 with spruce wood through cone calorimeter tests<sup>16</sup> and standard fire resistance tests.<sup>25,26</sup>  
 268 The in-depth char front propagation was measured for the entire width of the short panel as well as the  
 269 large panel by cutting the panels at every 5 cm height after each test and making direct measurements  
 270 of the char depth. The steps for cutting the panel are presented in Fig. 12 and the results are shown in  
 271 Fig. 13 and 14 in the form of contour plots for tests with burner powers of 10, 20, 30, and 50 kW and  
 272 exposure times of 15 and 30 minutes.

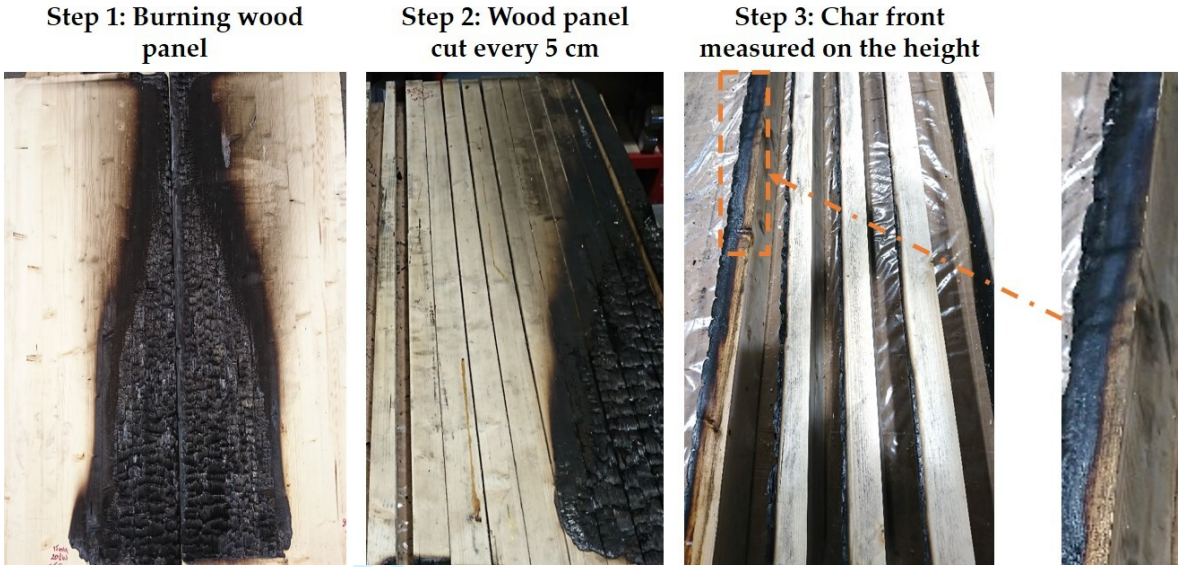


Figure 12: Steps for cutting the burning wood panel and measuring the location of the char front.

Figure 13 presents a comparison of the spatial profiles over the width of the char front depths on the short and large panels at the height of 60 cm for a test performed at 30 kW after 30 minutes of exposure.

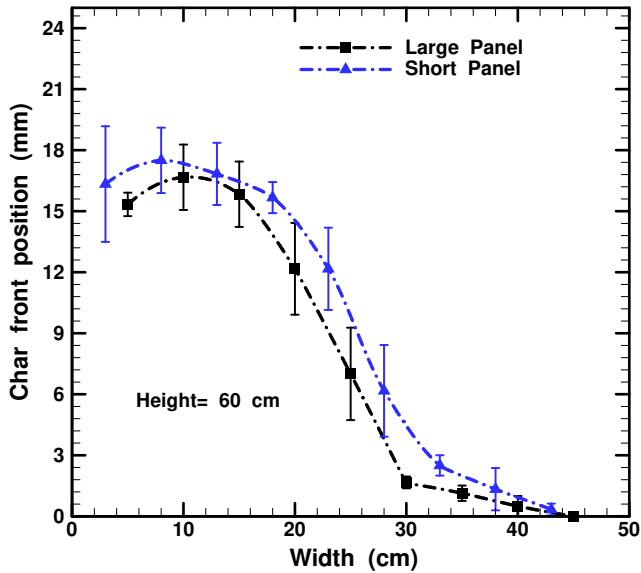


Figure 13: Comparison of the spatial profile over the width of the char front depths in the small and large panels after 30 minutes exposure to a 30 kW burner power.

The char front depth profiles shown in Fig. 13 confirm the observations made by Zeinali *et al.*<sup>5</sup>

1  
2  
3 276 regarding the different thermal exposure on the small and large panel. Indeed, the average char front  
4  
5 277 depths in the small panel are always slightly higher than those in the large panel, indicating that the short  
6  
7 278 panel receives a slightly stronger thermal exposure, and this holds true for the entire panel width. The  
8  
9 279 char front contours in Fig. 14 are based on experimental measurement (see protocol in Fig. 12). Thus,  
10  
11 280 each grid point corresponds to a direct measurement (at least 90 points per wood panel) and the contours  
12  
13 281 are plotted by interpolation between these data points. In addition, Fig. 14 suggests that the area of  
14  
15 282 charring on the wood panels is larger than the area of high heat fluxes observed on incombustible panels,  
16  
17 283 especially at higher heights near the corner. This is due to the additional heat flux provided by the burning  
18  
19 284 of the wood panels and the higher flame heights in these tests compared to the tests with incombustible  
20  
21 285 panels.<sup>5,7</sup>

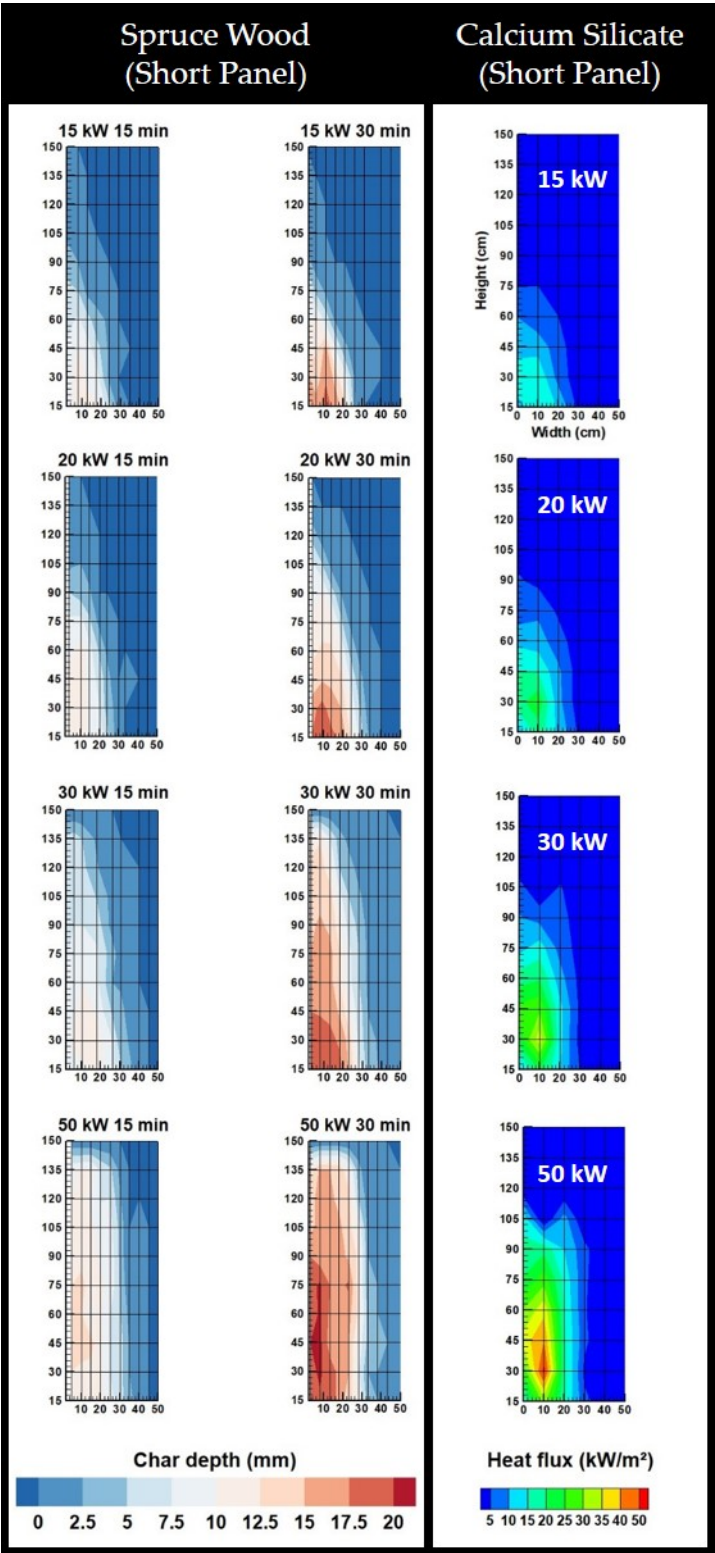


Figure 14: Contour plots of char front depths on a spruce wood panel (left) and contour plots of total heat fluxes on an incombustible panel (right) for burner powers of 15, 20, 30 and 50 kW.



### *Comparison of in-depth charring in SBI and cone calorimeter tests*

Some additional experiments with the cone calorimeter<sup>4</sup> were performed in order to compare the wood degradation in this setup with that observed in the SBI setup. For the SBI, the burner's heat fluxes have a highly non-uniform pattern over the panels (see Fig. 3), whereas the heat fluxes of the cone heater have a quite uniform pattern over the sample in cone calorimeter tests.<sup>4</sup> Moreover, according to Fig. 4, adding a combustible panel can greatly increase the local heat flux (for a 15 kW burner power, the local heat flux was equal to  $20 \text{ kW.m}^{-2}$  with the inert panel vs.  $35 \text{ kW.m}^{-2}$  with the wood panel). This makes it difficult to compare the results of cone calorimeter and SBI tests. Having that in mind, the in-depth char positions of the two scales as a function of the heat flux and the exposure time were compared. For that, the spruce wood samples were exposed to seven constant heat fluxes at the cone calorimeter without igniter, namely 20, 28, 35, 43, 50, 55 and  $60 \text{ kW.m}^{-2}$  for exposure times ranging from 15 to 30 min. It should be noted that the auto-ignition did not occur for each heat flux but in any case smoldering combustion (char oxidation and glowing) occurred. After each test, the samples were cut in their middle and the position of the char depth was measured with a ruler. Figure 15 shows a comparison of the char front positions obtained with the SBI at position 9 shown in Fig. 3 and the char front positions obtained with the cone calorimeter using either the heat flux measured with an inert panel (Fig. 15a) or the heat flux measured with a wood panel (Fig. 15b).



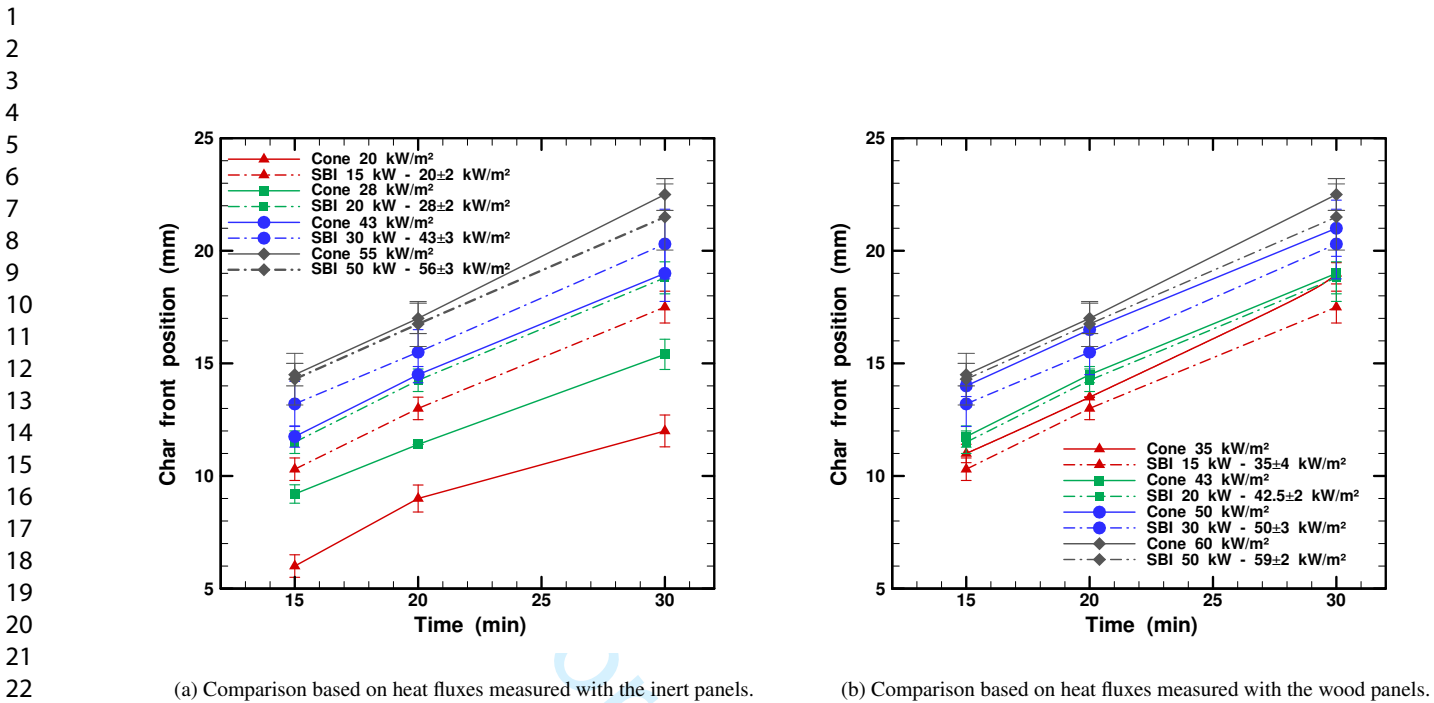


Figure 15: Comparison of the char front position between the cone and the SBI as a function of time, for different heat fluxes measured at position 9 shown in Fig. 3. The error bars indicate the magnitude of deviation across three repeatability tests, and the symbols indicate the average values.

In Fig. 15a, where the reference of heat flux is based on inert panels, the char depth positions in SBI and cone tests are in good agreement for the highest heat flux (showing differences less than 2 mm), although the two tests involve very different scales. Nevertheless, for the lowest heat fluxes (20 and 28 kW.m<sup>-2</sup>), the char front positions are no more comparable since for these burner powers the heat flux measured on a wood panel differs significantly from the heat flux measured on an inert panel, as shown in Fig. 4. This explains the extended char depth in the SBI tests. In Fig. 15b where the reference of heat flux is based on wood panels, the comparison of the char front positions obtained at the SBI scale and at the cone scale shows better agreement between the two scales. The deviations for each heat flux are less than 2 mm between the SBI and the cone tests. These comparisons show that it would be more accurate to consider the heat flux with the wood panel for studying the scaling effect. However, results also show that for heat fluxes measured on the inert panel greater than 43 kW.m<sup>-2</sup>, it is possible to consider that the positions of the char front will be similar between the two scales. At lower heat fluxes, the modification of heat flux due to the burning of the wood panel is too large to predict the panel degradation from only the heat flux map measured on an inert panel.

## CONCLUSIONS

The SBI was used to study the fire behavior of spruce wood at various burner powers and exposure times, i.e. beyond those defined in the standard of SBI.<sup>2</sup> Correspondingly, a total of 22 tests were performed with measurements including char depth, heat flux, in-depth temperatures with very thin thermocouples (0.1 mm diameter) embedded inside wood panels as well as position of the char on the exposed surface. The heat fluxes measured with inert panels provided data about the distribution of total incident heat fluxes over the panels for different burner powers. Accordingly, it was quantified how the heat flux distribution over the surface of the panels is non-uniform, with heat fluxes ranging from 1.5 to 50 kW.m<sup>-2</sup>. The measured heat fluxes with wood panel were up to 85 % higher than the heat fluxes with an incombustible panel. For the highest burner powers, the total heat flux measured over the combustible panels was predominantly due to the burner power, rather than the burning of the panels themselves. This causes the heat fluxes to converge to those observed with incombustible panels. Indeed for these burner powers, the flame has already reached its maximum thickness and thus the heat flux cannot increase further. Moreover, high burner powers induce strong opposite flow of pyrolyzate mass over the surface, causing a so-called 'blowing effect' that leads to convective cooling.<sup>22</sup>

As demonstrated in some recent studies, the in-depth temperature can be underestimated when the thermocouple is not fixed in an appropriate way. Very thin thermocouples implanted along the isotherms were used in this study to quantify this underestimation and to accurately measure the in-depth temperatures. As a result, it was found that the thermocouple wires implanted along the isotherms are faster to detect the rise of temperatures compared to the sheathed thermocouples placed in holes drilled from the back side, with up to 75 °C difference in the temperatures obtained using the two methods. Moreover, the position of the char front deduced from the 300 °C isotherm was found to comply very well with the direct measurements.

For the charring rate, a quasi-steady-state plateau between 0.6 and 0.7 mm.min<sup>-1</sup> was found while the propagation of the charring front on the exposed surface increased according to the exposure time and the burner power. In addition, it was found that the surface area of the highly degraded region varies linearly with the burner power for a fixed exposure time.

The comparison of the char front depth in the cone calorimeter and the SBI setup showed a good agreement for the higher heat fluxes. However, for the lower heat fluxes measured with an inert panel, there is a significant difference between the char front depths in SBI and cone tests, namely those of the SBI are

1  
2  
3 347 higher by nearly 100 % at an exposure time of 15 min, albeit the difference decreases to approximately 50  
4 348 % for exposure times above 20 min. This difference is mainly due to the presence of flaming combustion  
5 349 on the panels in the SBI tests. This suggests, for the study of the scaling change, to match the heat fluxes  
6 350 for the cone calorimeter with those of the SBI test obtained with the wooden panel. However, the results  
7 351 also show that when the heat fluxes are above  $43 \text{ kW.m}^{-2}$ , the heat fluxes measured with incombustible  
8 352 panels could be sufficient for the study of the change of scale.

15 353 **Declaration of conflicting interests**

18 354 The author(s) declared no potential conflicts of interest with respect to the research, authorship, and/or  
19 355 publication of this article.

23 356 **References**

26 357 [1] R. vanMierlo and B. Sette, “The single burning item (sbi) test method- a decade of development  
27 358 and plans for the near future,” *Heron*, vol. 50, no. 4, pp. 191–208, 2005.

30 359 [2] E. Standard, “13823: 2013 reaction to fire tests for building products—building products excluding  
31 360 floorings exposed to the thermal attack by a single burning item,” *AFNOR, ICS*, vol. 13, p. 50, 2002.

34 361 [3] ISO, “9705: International standard—fire tests—full-scale room test for surface products,” *Interna-  
35 362 tional Organization for Standardization, Geneva, Switzerland*, 1993.

39 363 [4] ISO, “5660-1: Reaction-to-fire tests – heat release, smoke production and mass loss rate – part 1:  
40 364 Heat release rate (cone calorimeter method) and smoke production rate (dynamic measurement).,”  
41 365 *International Organization for Standardization, Geneva, Switzerland*, 2015.

45 366 [5] D. Zeinali, S. Verstockt, T. Beji, G. Maragkos, J. Degroote, and B. Merci, “Experimental study of  
46 367 corner fires part i: Inert panel tests,” *Combustion and Flame*, vol. 189, pp. 472–490, 2018.

50 368 [6] J. Zhang, M. Delichatsios, and M. Colobert, “Assessment of fire dynamics simulator for heat flux  
51 369 and flame heights predictions from fires in sbi tests,” *Fire Technology*, vol. 46, no. 2, pp. 291–306,  
52 370 2010.

- [7] D. Zeinali, S. Verstockt, T. Beji, G. Maragkos, J. Degroote, and B. Merci, "Experimental study of corner fires part ii: Flame spread over mdf panels," *Combustion and Flame*, vol. 189, pp. 491–505, 2018.
- [8] D. Lipinskas and R. Mačiulaitis, "Further opportunities for development of the method for fire origin prognosis," *Journal of Civil Engineering and Management*, vol. 11, no. 4, pp. 299–307, 2005.
- [9] P. Van Hees, T. Hertzberg, and A. Steen-Hansen, "Development of a screening method for the sbi and room corner using the cone calorimeter," 2002.
- [10] A. S. Hansen and P. J. Hovde, "Prediction of time to flashover in the iso 9705 room corner test based on cone calorimeter test results," *Fire and materials*, vol. 26, no. 2, pp. 77–86, 2002.
- [11] M. A. Delichatsios, "Application of upward flame spread for the prediction of sbi and iso room corner (and parallel wall) experiments and classification," *Thermal Science*, vol. 11, no. 2, pp. 7–22, 2007.
- [12] T. Hakkarainen and M. A. Kokkala, "Application of a one-dimensional thermal flame spread model on predicting the rate of heat release in the sbi test," *Fire and Materials*, vol. 25, no. 2, pp. 61–70, 2001.
- [13] J. Axelsson, P. Andersson, A. Lonnermark, P. Van Hees, and I. Wetterlund, "Uncertainties in measuring heat and smoke release rates in the room/corner test and the sbi," *SP RAPPORTSTATENS PROVNINGSANSTALT*, vol. 2011:04, 2001.
- [14] J. Axelsson and P. Van Hees, "New data for sandwich panels on the correlation between the sbi test method and the room corner reference scenario," *Fire and Materials: An International Journal*, vol. 29, no. 1, pp. 53–59, 2005.
- [15] L. Tsantaridis, *Reaction to fire performance of wood and other building products*. PhD thesis, Bygghvetenskap, 2003.
- [16] L. Terrei, Z. Acem, V. Marchetti, P. Lardet, P. Boulet, and G. Parent, "In-depth wood temperature measurement using embedded thin wire thermocouples in cone calorimeter tests," *International Journal of Thermal Sciences*, p. 106686, 2020.

1  
2  
3  
4 397 [17] D. M. Chaudhari, G. J. Fiola, and S. I. Stoliarov, “Experimental analysis and modeling of buoyancy-  
5 398 driven flame spread on cast poly (methyl methacrylate) in corner configuration,” *Polymer Degradation and Stability*, vol. 183, p. 109433, 2021.  
6 399  
7  
8  
9  
10 400 [18] R. Fahrni, J. Schmid, M. Klippel, and A. Frangi, “Correct temperature measurements in fire exposed  
11 401 wood,” in *World Conference on Timber Engineering (WCTE 2018)*, pp. MAT–O9, ETH Zurich, Institute of Structural Engineering (IBK), 2018.  
12 402  
13  
14  
15  
16 403 [19] R. Fahrni, J. Schmid, M. Klippel, and A. Frangi, “Investigation of different temperature measure-  
17 404 ment designs and installations in timber members as low conductive material,” in *10th International Conference on Structures in Fire (SiF 2018)*, pp. 257–264, Belfast, United Kingdom, 2018.  
18 405  
19  
20  
21  
22 406 [20] P. Reszka and J. Torero, “In-depth temperature measurements in wood exposed to intense radiant  
23 407 energy,” *Experimental Thermal and Fluid Science*, vol. 32, no. 7, pp. 1405–1411, 2008.  
24  
25  
26  
27 408 [21] D. Drysdale, *An introduction to fire dynamics*. John Wiley & Sons, 2011.  
28  
29  
30  
31  
32 410 [23] D. Zeinali, *Flame spread and fire behavior in a corner configuration*. PhD thesis, Ghent University, 2019.  
33 411  
34  
35  
36 412 [24] H. C. Tran and R. H. White, “Burning rate of solid wood measured in a heat release rate calorimeter,”  
37 413 *Fire and materials*, vol. 16, no. 4, pp. 197–206, 1992.  
38  
39  
40  
41 414 [25] A. Frangi and M. Fontana, “Charring rates and temperature profiles of wood sections,” *Fire and*  
42 415 *Materials*, vol. 27, no. 2, pp. 91–102, 2003.  
43  
44  
45 416 [26] I. ISO, “834: Fire resistance tests-elements of building construction,” *International Organization*  
46 417 *for Standardization, Geneva, Switzerland*, 1999.  
47  
48  
49  
50  
51  
52  
53  
54  
55  
56  
57  
58  
59  
60